Progress In Electromagnetics Research C, Vol. 129, 143–155, 2023

Ultra-Wideband Flexible Wearable Antenna with Notch Characteristics for WLAN Applications

Amit Roy[1], Ashim K. Biswas[2], Arnab Nandi[1, *], and Banani Basu[1]

Abstract—This paper presents a narrow notch band, flexible, wearable ultra-wideband antenna built on a jeans substrate. Prior to designing the antenna, the dielectric properties of the jeans substrate are experimentally investigated. The effects of antenna shape and substrate loss characteristics on resonant performances are discussed with reference to the notch characteristics. The proposed antenna is shaped like a cumulative rugged element, with two identical legs. The investigation of the designed antenna shows the operating frequency ranges ($S_{11} \leq -10\,\text{dB}$) in 2.4–4.2 GHz and 5.86–10.7 GHz bands with notch properties in telemetry/ mobile communications (4.4–4.99 GHz) and WLAN (5.15–5.85 GHz) band. Additionally, the prototype is investigated under on-body conditions. Measured results are also included for the validation of the designed prototype.

1. INTRODUCTION

Ultra-wideband (UWB) technology is widely valuable for wireless links, biomedical-healthcare wireless schemes, communication systems, and various internal strategies [1]. In 2002, the usage of UWB technology in the frequency band of 3.1–10.6 GHz was commercialized by the Federal Communications Commission (FCC). Though UWB technology is widespread, the problem arises during frequency interference from other narrowband schemes similar to the 3.5/5.5 GHz WiMAX frequency band and 5.2/5.8 GHz WLAN frequency band. Therefore, single/multiple band-notched characteristics in UWB antennas are very demanding to avoid interferences and such effects [2–4]. In [5], a circularly polarized antenna exhibiting circular polarization at 2.4 and 9.8 GHz and linear polarization at 4.31 and 6.75 GHz is discussed. This structure shows impedance bandwidths of 2.13–3.02 GHz and 4.01–10.00 GHz. The single element, printed on an FR-4 substrate with a compact size of $.29\lambda \times .34\lambda \times .008\lambda$, offers a gain fluctuation of 1.4–5.7 dBi and a peak radiation efficiency of 92.3% [6]. These types of antennas effectively utilize notch bands to eliminate noises. Wearable notch band antennas will have a more significant influence because they are typically used for crucial and sensitive applications like health, telemedicine, and defence. Therefore, notch band wearable antennas are crucial to preventing distortion and noise from other sources.

A growing trend in wearable technologies and smart clothing, where flexible electronics may be incorporated into clothes, is a promising area of UWB communication. On-body antennas, which are placed on the skin and typically built into garments, are widely used for communication [7, 8]. Usually, plastics or textiles are chosen as substrate materials for flexible and wearable antennas [9]. Researchers like wearable antennas that are built into fabric materials [10]. Microstrip antennas are a good choice for on-body wearable applications as they possess several key attributes, such as simplicity in construction and reduced cost. Fabrics often have a reduced relative permittivity (< 2), suffer partly from trapped air, and have variable electrical characteristics because of moisture. Consequently, developing a textile antenna for wearable applications is a challenging field of research.

Received 5 November 2022, Accepted 18 January 2023, Scheduled 30 January 2023

* Corresponding author: Arnab Nandi (arnab@ece.nits.ac.in).
[1] National Institute of Technology Silchar, Cachar, Assam, India. [2] JIS College of Engineering, Kalyani, India.

Over the past few years, the importance of wearable antennas like printed flexible antennas and such devices has been growing increasingly. Consequently, there is a continuous and high potentiality for flexible microwave components. The investigation of these components needs particular focus rather than using conventional substrates. These components can perform a wide range of applications, specifically for wearable and medical applications. The compact antenna with high performance in a wearable system has a remarkable demand in emergency rescue in a crisis environment, physical training, medical care, telemedicine, health monitoring, and satellite applications [2, 11–14]. UWB technology is an emerging area that confirms reduced cost, high-speed and short-range communication schemes. Therefore, this technology can be an upright contender for wireless on-body systems with widespread research aspects in on-body broadcast networks [15]. The antenna made of textile material is easily bendable and can be incorporated into clothing and garments due to its high flexibility [16].

Recently, a lot of band-notched UWB antenna designs have been proposed. In [17], a compact UWB monopole reconfigurable antenna with notched band features is suggested. An open-ended slit is imprinted on the radiating patch to find the band-notch property. The antenna shows notch characteristics in the WiMAX and WLAN bands. The antenna is fabricated on an FR4 substrate with a dielectric constant of 4.4. Pin diode is utilized for switching purposes. A UWB antenna with conformal, planar, low-profile, and band-notched characteristics is presented in [18]. The antenna works from 3.8 to 8.3 GHz with a band rejection that extends from 5 to 6 GHz. It is designed with a polydimethylsiloxane (PDMS) substrate, having a permittivity of 2.77. In [19], a dual-band antenna operating in 1.71–2.69 GHz and 3.35–3.6 GHz is explored. The antenna is fabricated using a TLT-8 substrate with a dielectric constant of 2.55. It shows a notch at 2.7–3.34 GHz. A UWB antenna fabricated on a Taconic TLY-5A substrate ($\varepsilon_r = 2.17$) is presented in [20]. The antenna uses an electromagnetic band-gap (EBG) structure and shows the rejection characteristics on triple bands of 3.4–3.9 GHz, 5.15–5.825 GHz, and 7.25–7.75 GHz. In [21], a multiple-input multiple-output (MIMO) Vivaldi antenna printed on a Taconic RF-35 substrate working from 2.9 to 11.6 GHz with notch bands over 5.3–5.8 GHz and 7.85–8.55 GHz is explored. A UWB planar antenna with notch characteristics on 5.15–5.85 GHz is presented in [20]. The antenna is printed on a RO4003TM substrate with dielectric constant (ε_r) of 3.38. In [11], a compact UWB L-shaped slot-based antenna is explored. The antenna discards three frequency bands of 3.7–4.2 GHz, 5.15–5.825 GHz, and 7.25–7.75 GHz. During fabrication, an RT/duroid 6006 substrate with dielectric constant of 6.15 is used. In [22], a dual-notch UWB planar antenna with notches at 3.5 and 5.5 GHz is demonstrated. The antenna is fabricated using an FR4 substrate and utilizes a slitted EBG like mushroom-type structure for filtering action. A compact MIMO antenna with a band notch at WLAN (5.725–5.825 GHz) for UWB applications is presented in [16]. In [23], a dual-port graphene-based antenna printed on cotton fabric is discussed. In [24], a wearable UWB flexible antenna with a notch-band of 5.15–5.35 GHz is presented. The antenna is manufactured using an ultra-thin crystalline liquid polymer substrate with a dielectric constant of 2.9. A slot near feed location is utilized to achieve band notch characteristics.

In this article, a tiny UWB antenna suitable for the usage in challenging environments including wearable and bending circumstances is proposed. The band notch characteristic evades the telemetry/mobile communication (4.4–4.99 GHz) and WLAN (5.15–5.85 GHz) bands. This is done to keep it free from interference generated from similar or dissimilar systems. The antenna offers full UWB rejecting the telemetry/mobile communication and WLAN band in free space, wearable, and bending situations. Radiation characteristics and specific absorption rate (SAR) values are investigated and found appropriate for the single band-notched UWB antenna. Ansys Electronics 2021 R1 (Ansys) is used to simulate, analyse, and optimise the whole structure.

2. EVALUATION OF DIELECTRIC PROPERTIES

Prior to configuring the textile antenna, the dielectric characteristics of the jeans substrate are measured. A dielectric probe is utilized in this method of measurement, where the probe comprises a truncated transmission line segment. The propagated electromagnetic wave through the coaxial line is reflected back when the impedance is faced between the testing material and the probe. The fixed commercial software transforms the reflection parameters into dielectric parameters. The dry jeans sample is to be hard-pressed by the probe during the experiment. The field coupled with the probe fringes into

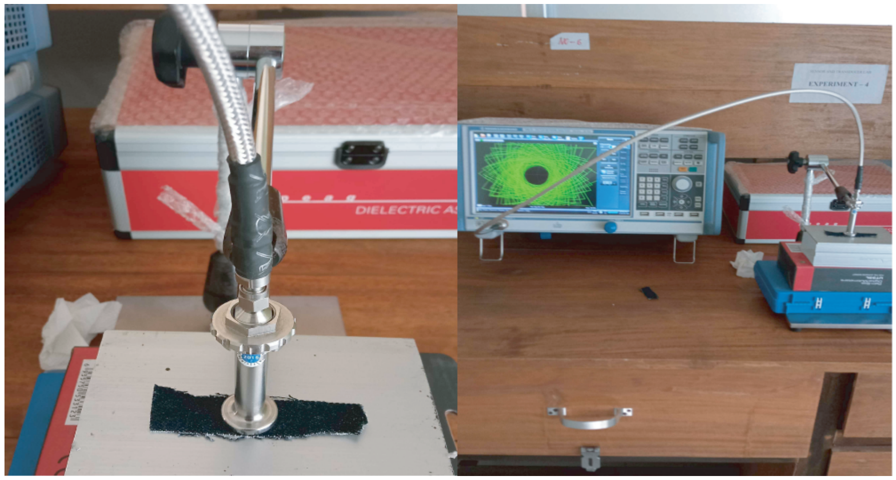

(a) (b)

Figure 1. Set up for dielectric properties measurement.

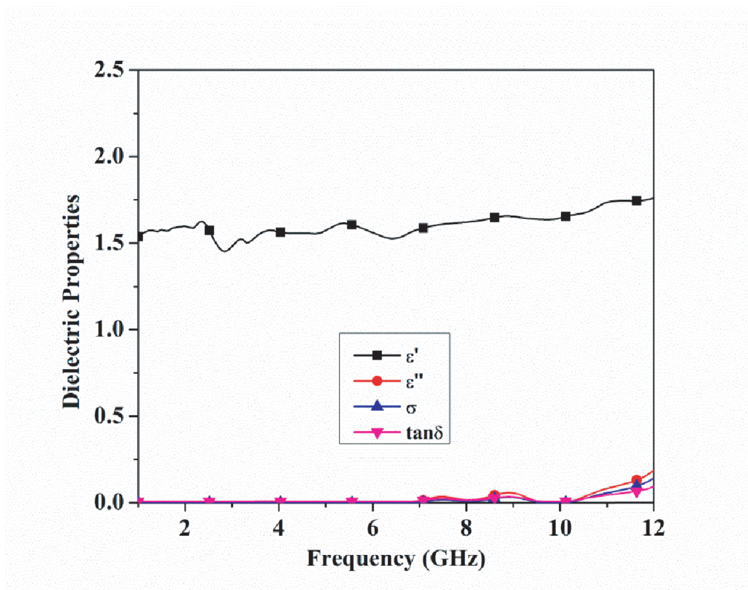

Figure 2. Dielectric properties of the jeans substrate.

the substrate to reform as they meet into the material. Then, the measured reflection parameters are transformed into the values of dielectric properties [25]. The dielectric properties of the substrate have been measured with the help of a Rohde & Schwarz (R&S) ZNB-20 vector network analyser and a Dielectric Assessment Kit (DAK)-3.5 probe over a wide frequency range. Dielectric properties measurement setup is shown in Fig. 1. The measured dielectric constant, loss factor, loss tangent, and conductivity of the jeans substrate are illustrated in Fig. 2. The average dielectric constant over the UWB range is around 1.6. The measured dielectric properties are utilized to design the textile antenna.

3. ANTENNA CONFIGURATION

Figure 3 represents the structure of the proposed antenna. The top and back surfaces are demonstrated in Figs. 3(a), (b), respectively. Two cumulative rugged-type elements are combined to form the radiator, where each element is a mirror image of the other. The antenna element is positioned on a readily

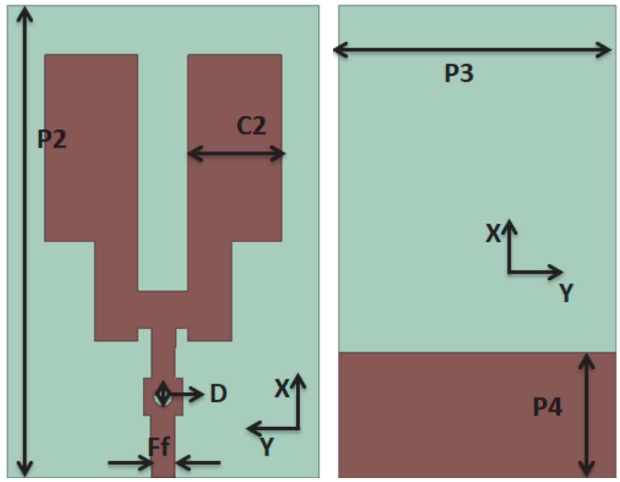

(a) (b)

Figure 3. (a) Top and (b) back views of the notch band UWB antenna.

available low-cost jeans substrate and fed with a 50-ohm microstrip line. The complete measured dielectric properties are used to design the antenna. Dielectric constant (ε_r) of 1.6, loss tangent ($\tan\delta$) of 0.02, and substrate thickness of 0.6 mm are utilized. Symmetrical tie-offs help to achieve impedance matching at the bases of the two rugged type elements, which are symmetric in nature. For effective impedance matching, two cut-off corners in the dimensions of the feed-patch junction are essential. The final antenna is designed after a systematic investigation. Notch band is created by the modification of feed line of the designed UWB antenna. A stopband characteristic is also produced. The stopband characteristic is linked through the tuning of the middle conductor and the established slots which are balanced around the axis of the patch antenna. A strong anti-phase current scattering appears beside the edges of the slot at the desired frequency. We have made different parametric variations to get the final antenna structure and checked the corresponding suitability. Some of these parametric tuneable conditions are discussed in the next section.

3.1. Parametric Design and Solution

First, a rectangular type antenna element is designed on a jeans substrate to operate in a wide frequency band with telemetry/mobile communications (4.4–4.99 GHz) and WLAN band notch characteristics. The antenna is designated as Antenna 1. Top and back views of the antenna are shown in Fig. 4. The investigation of this first antenna depicts the band range of 2.7–4.63 GHz, which is not found as suitable characteristics. Therefore, it is modified to keep the same ground plane.

A rectangular slot is cut at the middle to open a wide part of the patch on one side. The modified antenna is named as Antenna 2. The front view of the antenna is shown in Fig. 4. S_{11} (dB) curve illustrates that the frequency range over 2.65–4.76 GHz is also found unsatisfactory. Antenna 3 is designed by modifying Antenna 1 as shown in the figure. It is found by cutting two rectangular segments from both right and left sides on the upper portion of the primary patch. It offers a frequency range of 2.69–5.8 GHz. It also reflects no appropriate band deployment. Therefore, Antenna 4 is designed which is a combination of Antenna 2 and Antenna 3. The investigation of this antenna has been performed, and it is found that the response is not improved remarkably; some lacuna is still there. Another antenna designated as Antenna 5 is designed with the modification of Antenna 2. Two outer segments from both lower sides are removed. The investigation of this antenna shows a very wide band ranging from 2.4 to 11.25 GHz covering UWB (3.1–10.6 GHz) range. S_{11} (dB) for all the antennas (Antennas 1 to 5) are depicted in Fig. 4(b). In the current study, -10 dB is considered to demark the operating and notch bands. Antenna 5 is considered as the basic antenna. Modification on this antenna will be executed to convert it into a WLAN notch UWB antenna.

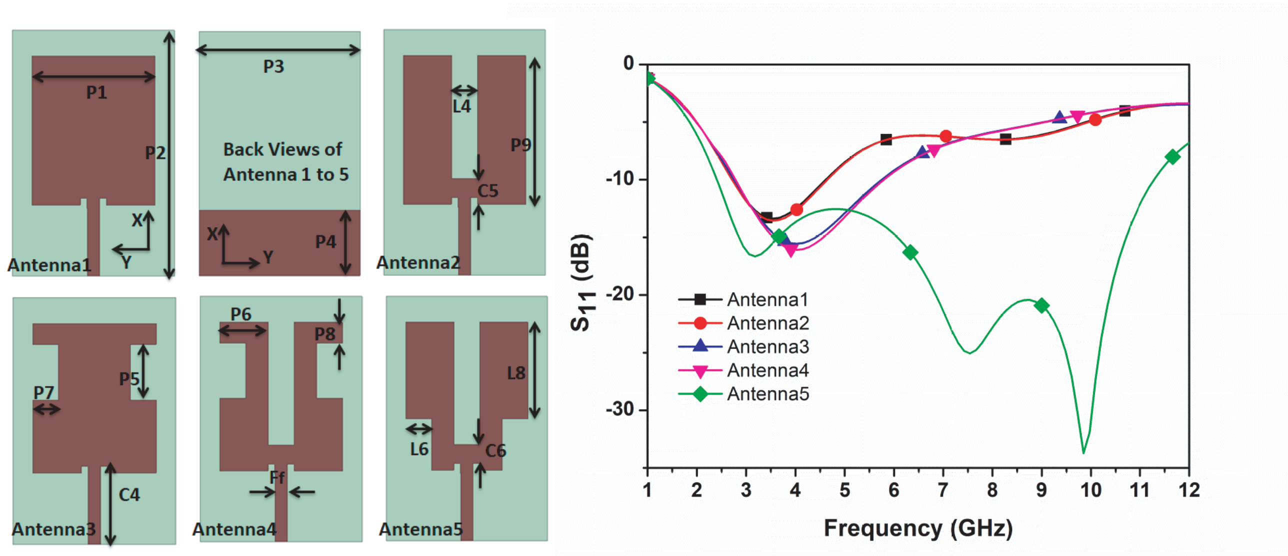

(a) (b)

Figure 4. (a) Evaluation steps to design an UWB antenna. (b) Return loss of antennas 1, 2, 3, 4, and 5.

3.2. Design of Single Band-Notched UWB Antenna

To reduce the interferences from the IEEE802.11a and WLAN systems, the functioning of band-notched property is desirable in a UWB system. For the creation of a notched band with WLAN (5.15–5.85 GHz) band, a filtering property is introduced using modification in the feed line of the designed UWB antenna. Four different modifications are illustrated here to demonstrate the process. Fig. 5 shows the geometry and dimensions of the UWB antenna with feed line modifications.

In configuration 1, a rectangular segment with a circular slot is established, as shown in Fig. 5(a). The structure uses $L1 = 3$ mm, $L2 = 4$ mm and slot diameter as 1.5 mm. The investigation shows that the configuration offers dual notches, but it is not very effective, and the operating bands are

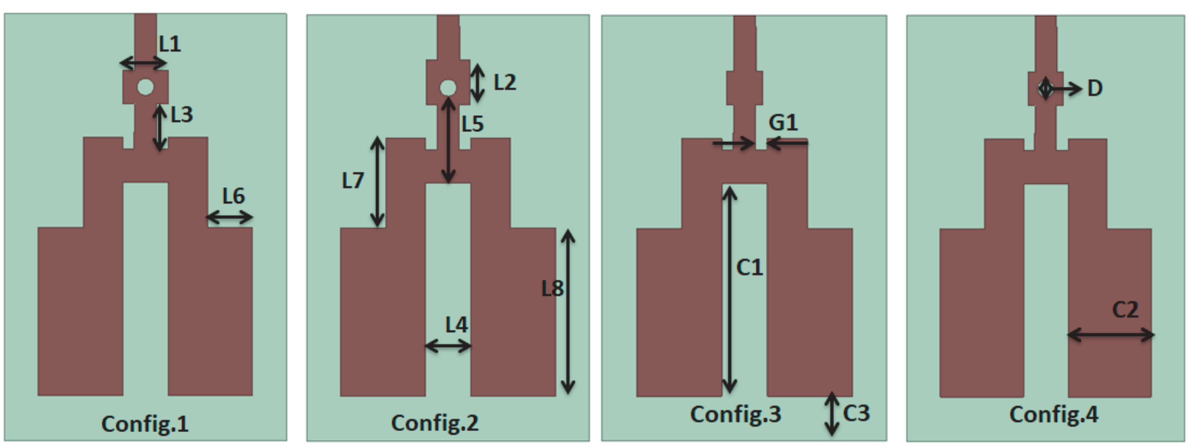

(a) (b) (c) (d)

Figure 5. Feed line modification steps to design the UWB antenna with telemetry/mobile communications and WLAN notch. (a) Config. 1: $L1 = 3$ mm, $L2 = 4$ mm with Circular Slot; (b) Config. 2: $L1 = 4$ mm, $L2 = 3.9$ mm with Circular Slot; (c) Config. 3: $L1 = 3$ mm, $L2 = 3.2$ mm without Circular Slot; (d) Config. 4: $L1 = 3$ mm, $L2 = 3.2$ mm with Circular Slot.

narrow. Therefore, configuration 2 is investigated where $L1 = 4$ mm, $L2 = 3.9$ mm with the same circular slot, which offers a single operating band causing exclusion of some portion of ultra-wideband. For the solution, variables $L1$ and $L2$ are again tuned to 3.2 mm and 3 mm, respectively. The circular slot is also removed. The investigation of this configuration offers good results compared to that of the previous one. To improve the resulting S_{11} (dB), the exact telemetry/mobile communication (4.4–4.99 GHz) and WLAN (5.15–5.85 GHz) are rejected, and a better passband is found. The antenna is further modified by tuning $L1$ and $L2$ to 3 mm and 3.2 mm respectively. Keeping the circular slot on the feed line, configuration 4 is investigated which offers improvement in results. The antenna covers the full UWB with telemetry/mobile communications (4.4–4.99 GHz) and WLAN band notch characteristics. Geometries for all these four configurations are demonstrated in Figs. 5(a)–(d). S_{11} (dB) curve is explored in Fig. 6(a). A study on stopband characteristics on the final modification is also done. The response is illustrated in Fig. 6(b). Here, it is clearly observed that telemetry/mobile communication (4.4–4.99 GHz) and WLAN (5.15–5.85 GHz) bands are placed in the stopband region. This result supports the significance of the final structure of the UWB notch antenna. The optimized dimensions of the antenna are explored in Table 1.

Table 1. Dimensions of the designed antenna.

Parameter	Dimension (mm)	Parameter	Dimension (mm)	Parameter	Dimension (mm)
$L1$	3.3	$L2$	3	$L3$	4.75
$L4$	4	$L5$	15	$L6$	4
$L7$	8	$C1$	19	$C2$	7.5
$C3$	4	$C4$	12	$C5$	4
$C6$	3	D	1.5	Ff	2
$G1$	1.05	$P1$	19	$P2$	38
$P3$	23	$P4$	10.2	$P5$	8.6
$P6$	7.5	$P7$	4	$P8$	3.2

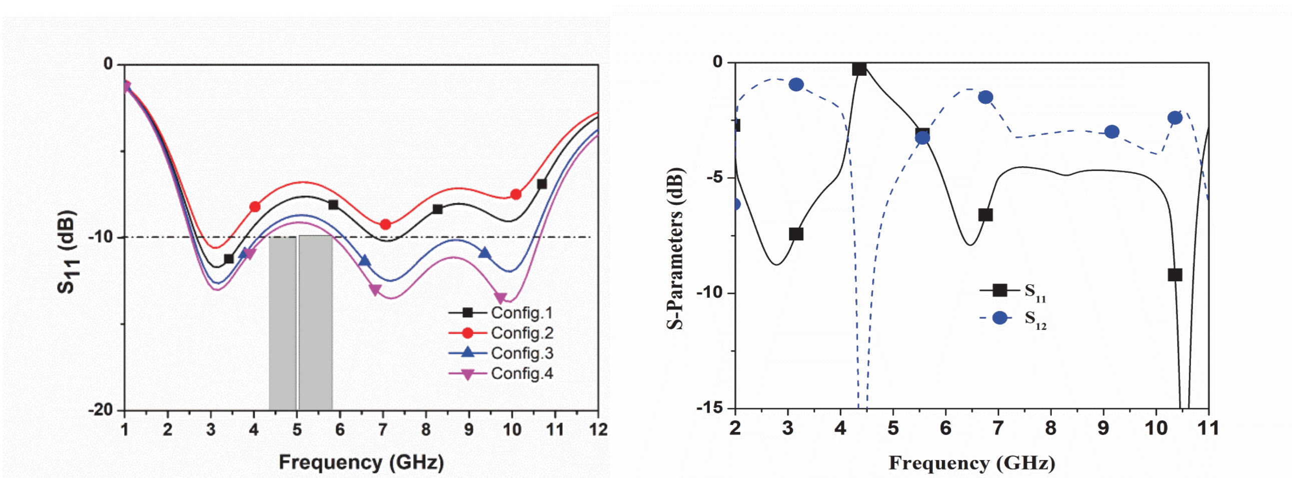

(a) (b)

Figure 6. (a) Return loss during modification of feed line of basic UWB antenna. (b) Normalized Stop band characteristics due to modification of feed line.

4. FABRICATION AND ANALYSIS OF ANTENNA PERFORMANCES

Two textile antennas without and with feed line modification are fabricated with the help of low thickness (about 0.07 mm) copper foil. The used jeans substrate is the same textile that is utilized to measure dielectric properties. Measured permittivity (ε_r) and thickness of the jeans as 1.6 and 0.6 mm are used. Both antennas are practically examined.

Figures 7(a) and (b) illustrate two textile antennas. Each antenna covers the volume about $23 \times 38 \times 0.6\,\text{mm}^3$. The antenna without feed line modification depicts S_{11} (in dB) less than 10 dB for the frequency band 2.4–11.25 GHz during the simulation and 2.33–11.3 GHz during measurement as shown in Fig. 8(a). Both the results confirm the full UWB (3.1–10.6 GHz) range. The initial antenna is modified to get a notch band over telemetry/mobile communications (4.4–4.99 GHz) and WLAN (5.15–5.85 GHz). Simulated S_{11} (dB) of this antenna offers the frequency ranges of 2.4–4.2 and 5.86–10.7 GHz, and measured results show the ranges of 2.35–4.22 and 5.94–11 GHz as presented in Fig. 8(b).

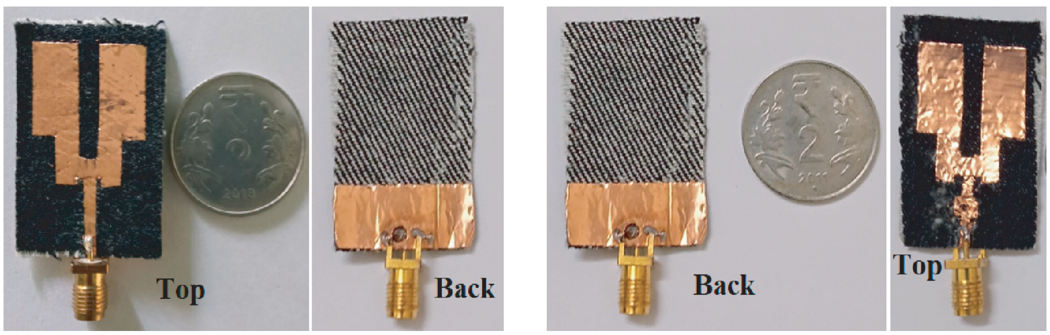

(a) (b)

Figure 7. (a) Return loss during modification of feed line of basic UWB antenna. (b) Normalized Stop band characteristics due to modification of feed line.

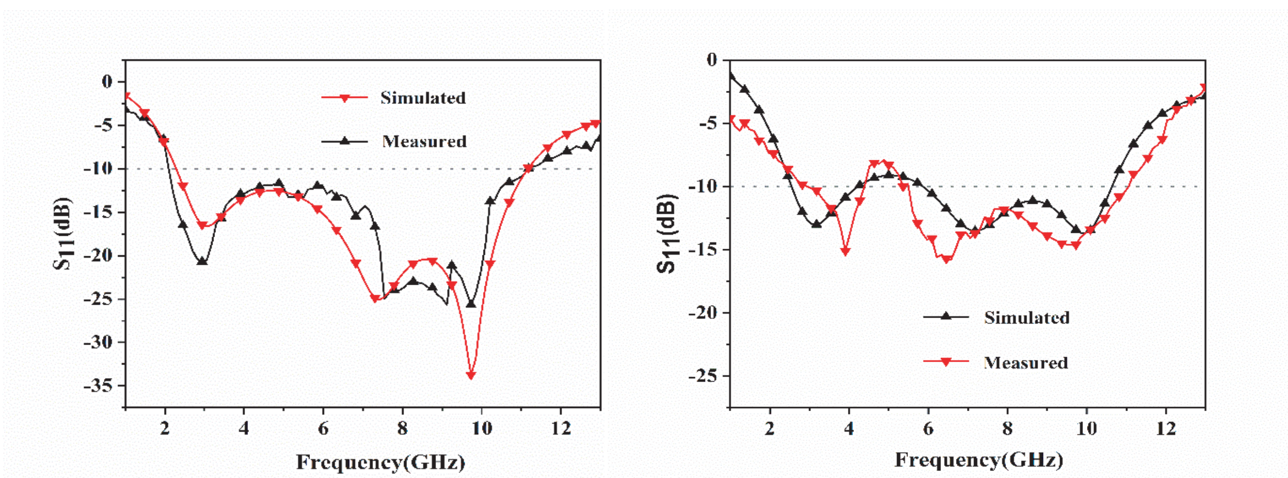

(a) (b)

Figure 8. S_{11} (dB) curve. (a) Basic UWB antenna. (b) Proposed UWB notch antenna.

4.1. Analysis of Surface Current Distribution

The current scatterings at different frequencies such as 5.5, 8, 8.5, and 10.6 GHz are investigated for the proposed textile prototype. Zero degree phases are considered for all current distributions. Fig. 9 displays all these current distributions. It is observed from the figure that at 5.5 GHz, the current

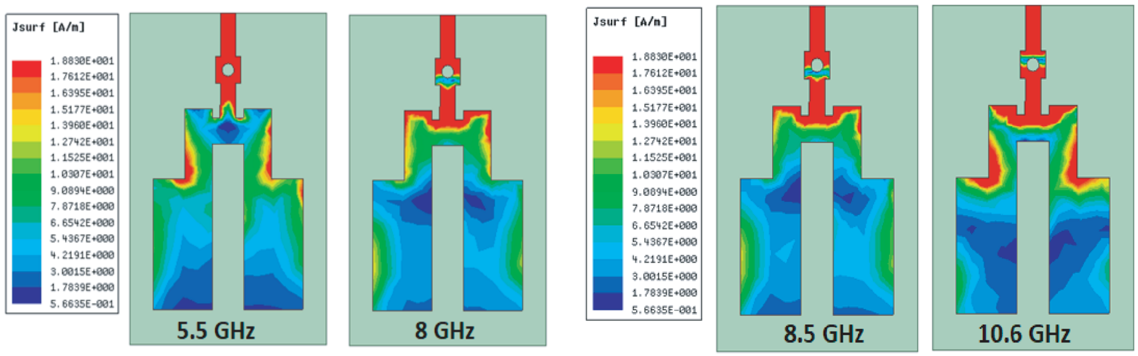

Figure 9. Surface current distributions of the proposed antenna at 5.5, 8, 8.5 and 10.6 GHz.

distribution is fairly restricted at the feed line with respect to other frequencies such as 8, 8.5, and 10.6 GHz. A band restriction with bands of 4.4–4.99 GHz and 5.15–5.85 GHz is established due to the formation of an optimized rectangular section with a circular slot on the feed line. The current scattering on the patch surface tends to accumulate near the defected zone. The existence of these band-notching assemblies is liable to the irregular scattering of antenna surface current and formation of notch-bands at several frequencies. The establishment of this band rejection helps to design the textile based single notch UWB antenna.

4.2. Radiation Properties

The proposed textile antenna is investigated in an anechoic chamber for far-field patterns. Both E- and H-plane simulated and measured patterns at 3.5, 8 and 10.6 GHz are illustrated in Figs. 10(a), (b), and (c). The simulated 3-D patterns in dBi scale for E-field at 3.5, 8, and 10.6 GHz are demonstrated in Fig. 10(d). The measured co and cross polarization patterns of the designed antenna are compared with the simulated patterns. A good agreement is found between these two. Slight dissimilarities occur at a few angles that correspond to the feeding cables, the positions of the SMA connectors, and alignment errors. It can be perceived from the patterns that for all the three frequencies cross-polarized radiations

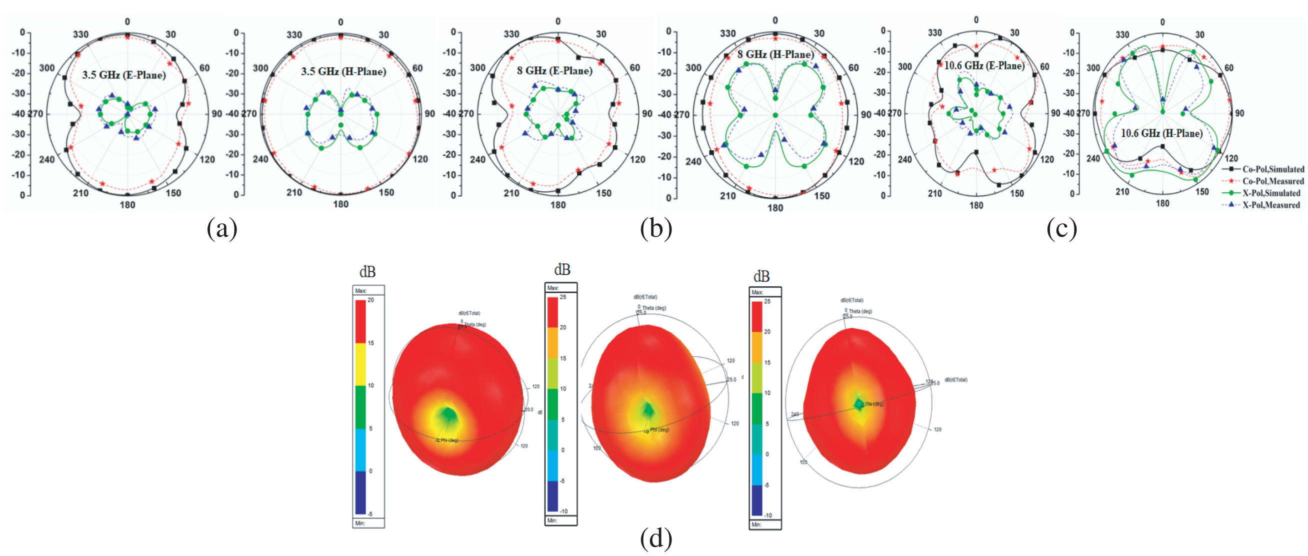

Figure 10. Normalized simulated and measured radiation patterns at (a) 3.5 GHz, (b) 8 GHz and (c) 10.6 GHz; (d) 3-D patterns for E-field at 3.5, 8 and 10.6 GHz.

are reduced with respect to that of co-pol patterns. Mainly unidirectional patterns are observed. These types of patterns are favourable for wearable antennas during their on-body attachment. The unidirectional radiation pattern can diminish the radiation energy concerning the human tissue. This helps to decrease the SAR value along with impacts of human body on the performance of the antenna (Wen 2018). Fig. 11 demonstrates the variation of gain and radiation efficiency with the frequency variation for the proposed antenna. The highest measured peak gain is about 4.8 dBi at 10.5 GHz in the application band. Radiation efficiency is $\geq 75\%$ throughout the operating band.

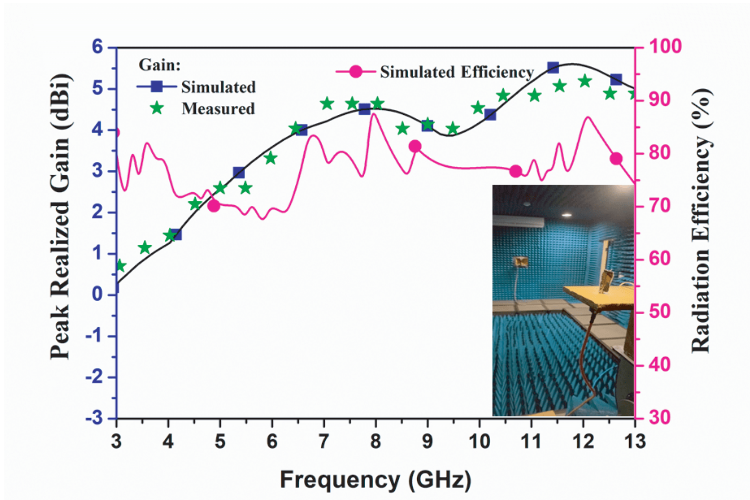

Figure 11. Variation of gain and radiation efficiency with frequency.

4.3. Bending Analysis

The prototype is bent and analysed considering different radii of curvatures as shown in Fig. 12(a). Generally, in antenna design, the parameter S_{11} is directly interrelated with the performance assessment of the antenna. This section has examined the tolerable nature of the proposed conformal antenna. We have considered the radii of 15, 18, and 20 mm for the investigation. Investigated S-parameters are illustrated in Fig. 12(b). The investigation revealed that the acceptable bending radius is 18 mm. For bending radius more than 18 mm, the proposed antenna satisfies the full UWB with notch over 4.4–4.99 GHz and 5.15–5.85 GHz. If the radius is (< 18) mm, it may disrupt the band specifications. A comparison with similar type works is depicted in Table 2.

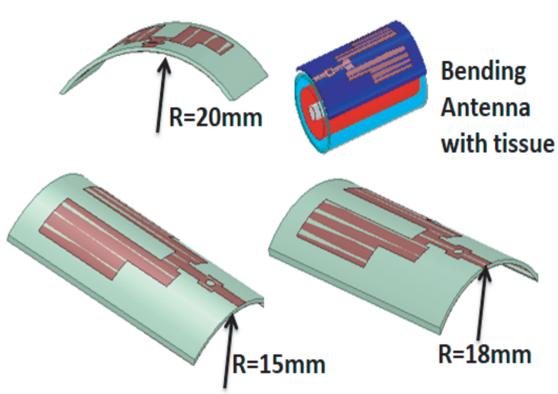

(a)

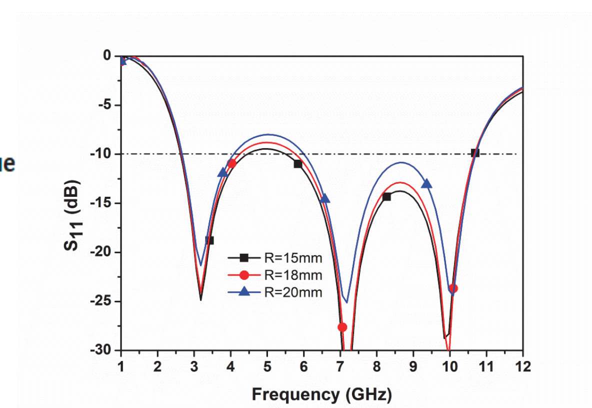

(b)

Figure 12. (a) The proposed antenna structure in bending conditions. (b) S_{11} (dB) curve of the proposed UWB notch antenna for bending conditions.

Table 2. Comparison with similar other works with UWB band.

Ref.	Antenna Size	Substrate	Antenna Type	Band Notch (GHz)	Band Notch method	Gain
[20]	$.30\lambda \times .24\lambda \times .01524\lambda$	RO4003TM, 3.38	Non-wearable	5.15–5.85	Two slits on patch	3.1 dBi
[22]	$.59\lambda \times .51\lambda \times .043\lambda$	TLT-8, 2.55	no	(2.7–3.34)	Parasitic element	3.7 dBi
[24]	$.31\lambda \times .18\lambda \times .008\lambda$	FR4, 4.4	Non-wearable	3.3–3.7 /5.1–6.5	Open-ended slot in patch	3.4 dBi
[11]	$2.025\lambda \times .008\lambda \times .127\lambda$	RT/duroid 6006, 6.15	Non-wearable	3.5 and 5.5	L-shaped slot on patch	2.9 dBi
[3]	$.30\lambda \times .024\lambda \times 0.1524\lambda$	RO4003TM, 3.38	Non-wearable	5.15–5.85	Two slits on patch	Not-mentioned
[19]	$.40\lambda \times .29\lambda \times .0067\lambda$	Taconic RF-35, 3.5	Non wearable	5.3–5.8 and 7.85–8.55	SRR	2.2 dBi
[17]	$.25\lambda \times .45\lambda \times .0382\lambda$	RT 5880, 2.2	wearable	5–6	Two rectangular slots and concentric rings	2.6 dBi
[21]	$40\lambda \times .29\lambda \times .0064\lambda$	GML 1000, 3.2	Non wearable	5–6	SRR on patch	2.4 dBi
[18]	$.24\lambda \times ..24\lambda \times .006\lambda$	Coconut Husk, 1.85	Non wearable	4–6	MIMO Array	2.8 dBi
[12]	$.36\lambda \times .18\lambda \times .009\lambda$	Jeans, 1.6	wearable	5 GHz and 5.8 GHz	Omnidirectional antenna	3.2 dBi
[13]	$.70\lambda \times .70\lambda \times .036\lambda$	PDMS, 2.77	Non wearable	5 GHz	Two rectangular slots and concentric rings	2.6 dBi
[26]	$.68\lambda \times .38\lambda \times .157\lambda$	RT DUROID, 5880	wearable	6.75 GHz	Monopole antenna	3.4dBi
[25]	$.36\lambda \times .56\lambda \times .015\lambda$	Jeans, 1.6	wearable	2–12.2 GHz	MIMO antenna	Not mentioned
proposed	$.23\lambda \times .38\lambda \times .006\lambda$	Jeans, 1.6	Wearable	4.4–4.99, 5.15–5.85	A circular slotted rectangular section on feed line	4.8 dBi

4.4. On Body Performances

To validate the designed antenna, the antenna prototype is tested in free space and on a human phantom. The effect of human tissue on the antenna's performance is simulated using a multi-layer model of human tissue. The prototype with the phantom is depicted in Fig. 13(a). The properties of the tissue are utilised in accordance with [14]. Simulated and measured S_{11} (dB) are shown in Fig. 13(b). The figure shows that the antenna operates between 2.46 and 4.15 GHz and 6.3 and 10.83 GHz according to the simulation results, whereas the measured results offer a range of 2.35 to 4.1 GHz and 6.2 to 10.9 GHz. There is a significant difference in the signal level received at passband (-15 dB) and notch band (-6 dB) and thus fairly distinguishable. Simulation for a 1 g average specific absorption rate (SAR) based on IEEE-Standard for a human arm at 100 mW power is also carried out and shown in Fig. 14. The SAR value is acceptable across the entire operating band.

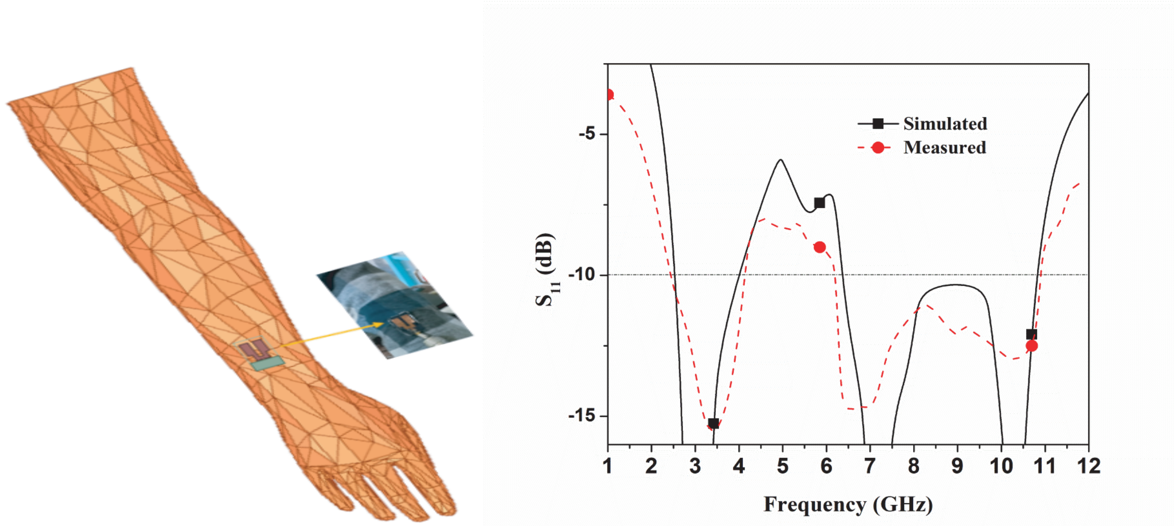

(a) (b)

Figure 13. Antenna in wearable situation: (a) Measured on wrist, (b) S_{11} curve of the proposed UWB notch antenna for on body conditions.

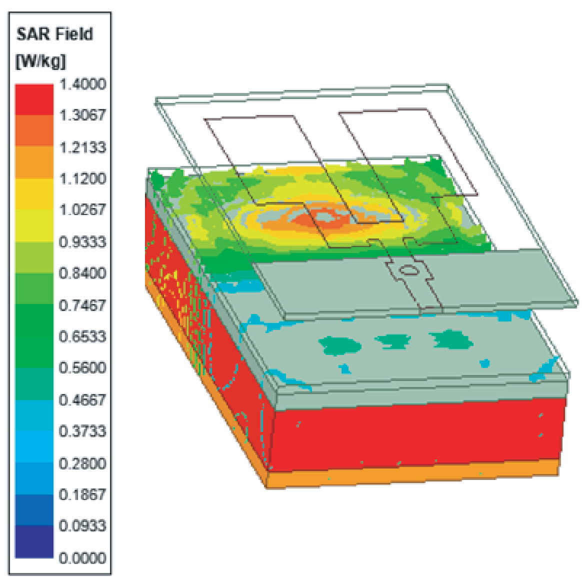

Figure 14. SAR value of the proposed antenna included with the human-body tissue model.

5. CONCLUSION

In this communication, a small, bendable textile antenna for wearable applications is demonstrated. The antenna is made up of two double-step rectangular sections connected by a microstrip line. It provides ultra-wideband coverage with notch characteristics over telemetry/mobile communication (4.4–4.99 GHz) and WLAN (5.15–5.85 GHz) bands. It offers dual bands ranging at 2.4–4.2 GHz and 5.86–10.7 GHz. The antenna is investigated for on-body use, and satisfactory results are obtained. The radiation characteristics are excellent. The gain and radiation efficiency of the proposed antenna are investigated. It is found that the highest peak gain is about 4.8 dBi at 10.5 GHz, and radiation efficiency is more than 75% throughout the application band. It is observed that the antenna can be bent without degrading its performance so long as the bending radius is greater than 18 mm. The SAR value under investigation is also within the acceptable range.

REFERENCES

1. Tang, M., H. Wang, T. Deng, and R. W. Ziowlski, "Compact planar ultrawideband antennas with continuously tunable, independent band-notched filters," *IEEE Transactions on Antennas and Propagation*, Vol. 64, 3292–3301, 2016.
2. Rekha, S. and G. S. Let, "Design and SAR analysis of wearable UWB MIMO antenna with enhanced isolation using a parasitic structure," *Iran J. Sci. Technol. Trans. Electr. Eng.*, Vol. 46, 291–301, 2022.
3. Du, Y., X. Yu, J. Siden, and G. Wang, "Design of sharp roll-off band notch with fragment-type pattern etched on UWB antenna," *IEEE Antennas and Wireless Propagation Letters*, Vol. 17, 2404–2408, 2018.
4. Li, Z., C. Yin, and X. Zhu, "Compact UWB MIMO Vivaldi antenna with dual band-notched characteristics," *IEEE Access*, Vol. 7, 38696–38701, 2019.
5. Kumari, S., Y. K. Awasthi, and D. Bansal, "A miniaturized circularly polarized multiband antenna for Wi-MAX, C-band & X-band applications," *Progress In Electromagnetics Research C*, Vol. 125, 117–131, 2022.
6. Subrahmanyam, V. G. and S. R. K. Kalva, "A novel UWB antenna with dual band notched characteristics using a single parasitic," *Progress In Electromagnetics Research C*, Vol. 125, 83–92, 2022.
7. Ma, L., R. M. Edwards, and W. G. Whittow, "A notched hand wearable ultra-wideband printed monopole antenna for sporting activities," *Loughborough Antennas & Propagation Conference*, London, 2008.
8. Wen, D., Y. Hao, M. O. Munoz, H. Wang, and H. Zhou, "A compact and low-profile MIMO antenna using a miniature circular high-impedance surface for wearable applications," *IEEE Trans. Antennas Propagation*, Vol. 66, 96–104, 2018.
9. Mohamadzade, B., R. B. V. B. Simorangkir, R. M. Hashmi, Y. Chao-Oger, M. Zhadobov, and R. Sauleau, "A conformal band-notched ultrawideband antenna with monopole-like radiation characteristics," *IEEE Antennas and Wireless Propagation Letters*, Vol. 19, 203–207, 2020.
10. Kittur, A. R. and L. Balaji, "Design of tri-band textile fractal antenna using three different substrate materials for Wi-Fi applications," *Progress In Electromagnetics Research C*, Vol. 120, 27–44, 2022.
11. Biswas, A. K., B. Basu, and A. Nandi, "Compact wearable UWB MIMO antenna with reduced mutual coupling and notch characteristics of WLAN band," *Arabian Journal Science Eng.*, 2022.
12. Khalili, F. K., A. Shahriari, and F. A. Haghshenas, "Simple method to simultaneously increase the gain and bandwidth of wearable antennas for application in medical/communications systems," *International Journal of Microwave and Wireless Technologies*, Vol. 13, 374–380, 2021.
13. Koo, T. W., Y. Z. Hong, Z. Park, K. Shin, and J. G. Yook, "Extremely low-profile antenna for attachable bio-sensors," *IEEE Trans. Antennas Propagation Letters*, Vol. 63, 1537–1545, 2015.
14. Shankar, S. and D. K. Upadhyay, "A compact maple leaf and triangular hybrid fractal shaped UWB frequency reconfigurable antenna with wide continuous tunable band notch," *Iran J. Sci. Technol. Trans. Electr. Eng.*, 2022.
15. Yang, T., D. Wa, and W. L. Stutzman, "Wearable ultra-wideband half-disk antennas," *Antennas and Propagation Society International Symposium*, Vol. 3A, 500–503, IEEE, 2005.
16. Masoodi, I. S., I. Ishteyaq, K. Muzaffar, and M. L. Magray, "A compact band-notched antenna with high isolation for UWB MIMO applications," *International Journal of Microwave and Wireless Technologies*, Vol. 13, 634–640, 2021.
17. Han, L., J. Chen, and W. Zhang, "Compact UWB monopole antenna with reconfigurable band-notch characteristics," *International Journal of Microwave and Wireless Technologies*, Vol. 12, 252–258, 2020.
18. Kerkhoff, A. and H. Ling, "A parametric study of band-notched UWB planar monopole antennas," *Antennas and Propagation Society International Symposium*, Vol. 2, No. 6, 1768–1771, IEEE, 2004.

19. Fu, S., Z. Cao, X. Quan, and C. Xu, "A broadband dual-polarized notched-band antenna for 2/3/4/5G base station," *IEEE Antennas and Wireless Propagation Letters*, Vol. 19, 69–73, 2020.
20. Abbas, A., N. Hussain, J. Lee, S. G. Park, and N. Kim, "Rectangular notch UWB antenna using EBG and SRR," *IEEE Access*, Vol. 9, 2508–2515, 2021.
21. Hammache, B., A. Messai, I. Messaoudene, and T. A. Denidni, "Compact ultra-wideband slot antenna with three notched-band characteristics," *Int. J. RF Microw. Computer Aided Eng.*, Vol. 30, 22146, 2020.
22. Alizadeh, F., C. Ghobadi, J. A. Nourinia, and M. B. Hamed, "UWB dual-notched planar antenna by utilizing compact open meander slitted EBG structure," *AEU — International Journal of Electronics and Communications*, Vol. 136, 153–175, 2021.
23. Kumar, J., B. Basu, F. Talukder, and A. Nandi, "Multimode-inspired low cross-polarization multiband antenna fabricated using graphene-based conductive ink," *IEEE Antennas wireless and Propagation Letters*, Vol. 17, No. 10, 1861–1865, October 2018.
24. Abbasi, Q. H., M. U. Rehman, X. Yang, A. Alomainy, K. Qaraqe, and E. Serpedin, "Ultrawideband band-notched flexible antenna for wearable applications," *IEEE Antennas and Wireless Propagation Letters*, Vol. 12, 1606–1609, 2013.
25. Biswas, A. K. and U. Chakraborty, "Compact wearable MIMO antenna with improved port isolation for ultra-wideband applications," *IET Microwaves, Antennas and Propagation*, Vol. 13, No. 4, 498–504, 5599.
26. Kim, Y. and K. H. Do, "Planar ultra-wideband slot antenna with frequency bandnotch function," *Antennas and Propagation Society International Symposium*, Vol. 2, 1788–1791, IEEE, 2004.